



STANFORD RESEARCH INSTITUTE
Menlo Park, California 94025 · U.S.A.

February 1, 1977

Quarterly Progress Report: PERC-0060-6
Covering the period 1 October to 31 December 1976

MASTER

SULFUR POISONING OF CATALYSTS

By: W. E. Isakson, K. M. Sancier, P. R. Wentzcek, H. Wise and B. J. Wood

Prepared for:

U.S. ENERGY RESEARCH AND DEVELOPMENT ADMINISTRATION
Chicago Operations Office
9800 Cass Avenue
Argonne, Illinois 60439

Attention: Daryl B. Morse
Sr. Contract Administrator

Contract No. E(36-2)-0060
SRI Project 4387

NOTICE
This report was prepared as an account of work sponsored by the United States Government. Neither the United States nor the United States Energy Research and Development Administration, nor any of their employees, nor any of their contractors, subcontractors, or their employees, makes any warranty, express or implied, or assumes any legal liability or responsibility for the accuracy, completeness, or usefulness of any information, apparatus, product or process disclosed, or represents that its use would not infringe privately owned rights.

Approved:

R. W. Bartlett for R. W. B.

R. W. Bartlett, Director
Materials Research Center

DISTRIBUTION OF THIS DOCUMENT IS UNLIMITED eb

CONTENTS

I	INTRODUCTION	1
II	FISCHER-TROPSCH CATALYSTS	2
	A. Kinetic and Magnetic Studies	2
	1. Experimental Program	2
	2. Experimental Results	3
	3. Discussion	7
	B. Chemical Activity of Surface Intermediates	11
	C. Carbon Deposition Boundaries for the C-H-O System in the Presence of Iron	14
III	METHANOL-SYNTHESIS CATALYSTS--SURFACE SULFIDATION AND SEGREGATION	16
IV	FUTURE WORK	18
V	REFERENCES	19

TABLES

1	Reduction of Catalysts B-2 and B-6 in 100% H ₂ at 1 Atmosphere	20
2	Isothermal Carburization Studies with Fischer-Tropsch Catalysts	21
3	Temperature-Programmed Carburization Studies with Catalysts B-2 and B-6	22
4	Observed Curie Temperature and Probable Assignments to Ferromagnetic Phases	23
5	Thermomagnetic Analysis of Fischer-Tropsch Catalysts B-2 and B-6 After Short-Term Carburization	24

6.	Thermomagnetic Analysis of Fischer-Tropsch Catalyst B-6 After Long Term Carburization	25
7.	Thermomagnetic Studies of Used Fischer-Tropsch Catalysts	26
8.	Interpretation of Thermomagnetic Measurements	27

ILLUSTRATIONS

1.	Mass Gain of Catalyst B-2 During Carburization in $H_2/CO = 3/1$ at 1 Atm	28
2.	Parabolic Plot of Mass Gain of Catalyst B-2 During Carburization in $H_2/CO = 3/1$ at 1 Atm	29
3.	Mass Gain of Catalyst B-2 During Long-Term Carburization in $H_2/CO = 3/1$ at 1 atm	30
4.	Percent Iron as a Function of Carbon/Iron During Carburization of Catalyst B-2 at 598 K	31
5.	Product Distribution as a Function of Temperature. Catalyst B-6 Carburized in $H_2/CO = 3$ at 673 K	32
6.	Iron-Oxygen-Graphite Phase Diagram 723 K, 1 Atm	33
7.	Scanning Electron Micrographs of Pressed Wafer of C79-1 Methanol Synthesis Catalyst	34

I INTRODUCTION

This study, performed under ERDA Contract E(36-2)-0060, concerns the deactivation of catalysts used to produce fuels from carbon monoxide and hydrogen. During this reporting period, we have shifted the major emphasis of the study from sulfur poisoning of methanol-synthesis catalysts to the role of carbon in Fischer-Tropsch catalysts. This direction of the study conforms to the original proposal as modified in recent discussions with the project Technical Monitor.

II FISCHER-TROPSCH CATALYSTS

A. Kinetic and Magnetic Studies

1. Experimental Program

We have used thermogravimetric and thermomagnetic techniques to study carbon deposition and removal on Fischer-Tropsch catalysts exposed to syn gas. The catalysts used in the kinetic studies were Fischer-Tropsch catalysts B-2 and B-6 provided by PERC-ERDA. The apparatus and procedures used in these studies were described in a previous progress report.¹ In the carburization studies, we ground and screened the catalyst samples (80% in the range of 20 to 60 mesh) and then reduced them in H_2 flowing at $100 \text{ cm}^3 \text{ min}^{-1}$ while increasing the temperature linearly from approximately 150 K to 725 K in about 16 hr. We then carburized the catalysts in H_2/CO under isothermal conditions in the temperature range 475 K to 600 K, or under nonisothermal conditions with linearly increasing temperatures from approximately 450 K to 600 K at rates varying from 0.37 K min^{-1} to 0.63 K min^{-1} . In most experiments, we adjusted the H_2/CO ratio to 3/1 (by volume); however, in one experiment, the H_2/CO ratio was 1.5/1 (by volume). One sample of B-6, after the temperature-programmed carburization, was exposed to H_2/CO (3/1) for 72 hr at 598 K. From one partially carburized sample of B-6 carbon was removed by heating the sample isothermally in flowing H_2 at several temperatures in the range 600 K to 720 K; this sample was later recarburized. Sample mass, temperature, and magnetization were monitored during carburization and reduction.

After carburization, the samples were cooled in He, then analyzed in situ by thermomagnetic analysis (TMA) in the temperature range 300 to

930 K. During the long-term carburization study, TMA was performed after 5, 26, 47, and 72 hr of carburization and with the temperature lowered from 598 to about 400 K to avoid the phase transitions that occur at higher temperatures. We also analyzed by TMA three catalyst samples that had been used by ERDA-PERC for Fischer-Tropsch synthesis studies at elevated pressures.² Samples of fused iron catalyst CCI-C73-2-01 and Raney iron catalyst, after reduction in H₂ and conditioning had been onstream for 100 hr in syn gas with H₂/CO ratios ranging from 2/1 to 3/1, at pressures ranging from 300 to 1000 psig, and at temperatures from 598 K to 648 K.² Another sample of catalyst CCI-C73-2-01 had been exposed to syn gas for several hours during which treatment carburization occurred.

2. Experimental Results

(a) Catalyst Reduction

Several samples of catalysts B-2 and B-6 were reduced in H₂ at a linear rate of temperature rise. The mass-loss data are presented in Table 1. Catalysts B-2 and B-6 show two differences: At comparable linear heating rates, the maximum rate of mass loss occurred at a higher temperature (T_{max}) for catalyst B-2 than for B-6, and the fraction of mass lost was somewhat lower for catalyst B-2 than for B-6.

(b) Isothermal Carburization Studies

Several samples of catalyst B-2 were exposed to CO/H₂ (3/1) mixtures at different temperatures and their weight gain recorded as a function of exposure time. Typical relative changes in catalyst mass due to carbon deposition are plotted in Figure 1. Carburization times were short (2 hr) in the study of bulk carburization. A time correction of 1 1/2 minutes (~ 10 dilution volumes) was applied to the data for the replacement of He carrier gas by the H₂/CO mixture. As noted previously, the carburization kinetics can be interpreted in terms

of a parabolic rate law with two regions, an early region (I) with a relatively high rate and a later region (II) with a much lower rate (Figure 2 and Table 2). At the same temperature, the carburization rates of catalysts B-2 and B-6 in region I are similar in magnitude. In region II, some differences become apparent. Similarly, changing the H_2/CO ratio from 3/1 to 1.5/1 does not alter the carburization behavior of catalyst B-6 (Table 2) except that the high initial rate of carburization (region I) persists somewhat longer at the higher H_2/CO ratio.

During the long-term exposure of catalyst B-6 to H_2/CO (3/1) at 598 K for 72 hr, after 4 hr of temperature-programmed carburization (425 to 598 K), the rapid mass increase (relative to the mass of the reduced catalyst) during the initial 10 hr was followed by a slower constant rate of mass increase (Figure 3). The temperatures are also recorded in the figure. The break at which the change in rate occurs corresponds to a mass increase approximately equivalent to stoichiometric Fe_2C , as noted on the ordinate scale. The times at which TMA were made are also marked in the Figure. Before the TMA measurements, the flowing syn gas was replaced by He and the temperature lowered from 598 to about 400 K.

(c) Temperature-Programmed Carburization Studies

In a series of experiments, we measured the total mass gain of catalysts B-2 and B-6 during carburization in the temperature range 440 K to 590 K at different linear rates at temperature rise. The results indicate little variation in relative mass gain as a function of heating rate (Table 3).

(d) Thermomagnetic Analysis (TMA) of Carburized Catalysts

All the catalysts were subjected to TMA in flowing He without exposing the samples to air after carburization. The force

exerted on the sample by the magnetic field is a function of the magnetization value of a specific phase present in the sample and its mass. Our studies indicate that for the carburized B-2 and B-6 catalysts, saturation magnetization is essentially reached at 2.0 to 2.5 kOe. We chose a magnetic field of 2.5 kOe for the TMA, to minimize contributions from paramagnetic components in the sample and to sharpen the Curie-point transitions. The magnetic force measurements were normalized to a gradient-coil current of 1.00 A.¹ Regardless of the carburization conditions, the observed Curie temperatures of B-2 and B-6 fell into several distinct temperature ranges, as shown in Table 4, where we have included the ferromagnetic phases assigned to reported¹ Curie temperatures.

From the TMA, we semiquantitatively estimated the amounts of the observable ferromagnetic phases. Although the results were corrected for the saturation magnetization and molecular weight of each phase,³ they represent approximations, because some of the iron phases may be too small to be detectable magnetically or may not be ferromagnetic. To estimate the amount of α -Fe in a sample, we considered the reaction $\text{Fe} + \text{Fe}_3\text{C} = \text{Fe}_2\text{C}$ (Hagg). The occurrence of this reaction is manifested by the nearly linear decrease of magnetic force observed during TMA as the temperature is raised from 650 to 900 K. The amount of Fe_3C in the specimen is estimated from TMA at lower temperatures (478 to 493 K) where the above reaction is unimportant.

Short-term carburization produced composition changes in the ferromagnetic phases of catalysts B-2 and B-6 (Table 5). Carburization at higher temperatures (> 500 K) led predominantly to the Hagg carbide. However, the relative amounts of the other phases depended on the initial composition of the catalyst and the carburization conditions. In general, Hagg carbide is the ferromagnetic phase favored by carburization at elevated temperatures. At temperatures below 500 K, hexagonal

Fe_2C is produced, as shown for B-2 (Table 5) and as found earlier¹ for B-6.

The results of long-term carburization of B-6 show that the Fe_3C produced in the early carburization was later converted to Hagg carbide (Table 6). Also, the carburization resulted in substantial carbon deposits as indicated by total mass changes greater than those required to produce Fe_2C . The TMA data in Table 6 were taken during the carburization study shown in Figure 3.

Table 7 gives the TMA results for the Raney iron sample, the fused iron CCI-C73-2-01 sample, and the B-6 catalyst sample. The Raney iron pellets, showed weak ferromagnetism at 300 K, with the total force at saturation magnetization of 6×10^{-4} dyne mg^{-1} sample. The magnetization showed no dependency on field strength above 1.5 kOe, indicating that paramagnetic components were not present. The major ferromagnetic phase was found to be Fe_3O_4 with smaller amounts of Fe_2C (Hagg) and $\alpha\text{-Fe}$. Heating the sample in He to 850 K and cooling it to 300 K for approximately 1.2 hr caused a small increase in the saturation magnetization (7×10^{-4} dyne mg^{-1} sample). However, for the sample that had been carburized for several days, the magnetization as a function of applied field at 300 K showed saturation at 2 kOe and a saturation magnetization force of larger magnitude, 0.28 dyne mg^{-1} sample. The results indicated the presence of only one ferromagnetic phase, Fe_3O_4 which was confirmed by x-ray analysis. A paramagnetic component was detected in this sample from the slope of 3.7×10^{-3} dyne mg^{-1} kOe⁻¹ above 2 kOe.

TMA of the fused iron catalyst CCI-C73-2-01, which had been carburized for several hours at 300 K exhibited saturation magnetization at 2 kOe with a resulting force of 1.0×10^{-2} dyne mg^{-1} . Above 2 kOe a paramagnetic phase was detected with gradient of 1.4×10^{-3}

dyne mg^{-1} kOe^{-1} . After heating the sample in He at 900 K for 5 min and cooling it to 300 K we observed an increase in magnetization force at 2 kOe to 2.2×10^{-3} dyne mg^{-1} . A second TMA showed that the heat treatment had caused changes in the Fe_3O_4 phase, whereas the α -Fe phase had remained unaffected, suggesting formation of larger ferromagnetic domains of Fe_3O_4 which exhibit greater magnetization.

Finally, we performed a long-term carburization study of catalyst B-6 at 1 atmosphere. This catalyst was reduced in H_2 for 16 hr at 575 K and 2 hr at 725 K, then carburized at 1 atm in H_2/CO (3/1) for several hours at 575 K. The catalyst was then treated with H_2/CO (3/1) for several days at temperatures between 575 K and 675 K (cf. Figure 3 and Table 6). TMA at 300 K indicated that the magnetization force at 2.5 kOe was large, 0.53 dynes mg^{-1} and due entirely to Hagg Fe_2C (Table 7).

3. Discussion

The experimental results of our studies of Fischer-Tropsch catalysts provide some information on the mechanism of the bulk processes involved in their reduction and carburization. From the variation of the temperature (T_{max}) at which the reduction rates reach their maxima as a function of linear heating rate, we can derive an activation energy for this process.⁴ Based on such an analysis, we find an activation energy for reduction of the iron oxide-based, low-silica catalyst B-6 of about 2 kcal mol^{-1} and for high-silica B-2, about 5 kcal mol^{-1} . The narrow range of heating rates used, limits the precision of these results. However, they suggest a difference in the case of reduction between B-2 and B-6. In addition, the low activation energies observed indicate a diffusion-limited process in which undoubtedly lattice-oxygen is transported from the bulk to the surface.

The parabolic law kinetics associated with the carburization process exhibit some small but finite differences between B-2 and B-6. For B-2 the activation energy for carburization during region I is about $11.5 \pm 1.5 \text{ kcal mol}^{-1}$ compared with $9.5 \pm 1.5 \text{ kcal mol}^{-1}$ for B-6.¹ For carburization during region II, the activation energies are $2 \pm 2 \text{ kcal mol}^{-1}$ for B-2 compared with $6 \pm 2 \text{ kcal mol}^{-1}$ for B-6. These differences in activation energies are probably related to differences in composition. The B-2 catalyst contains iron predominantly in the 2+ valence state; B-6 has a higher proportion of Fe^{3+} relative to Fe^{2+} . In addition, the presence of SiO_2 in B-2 may play a role in the carburization process.

To determine the stoichiometry of the iron carbide phases produced, we measured both sample magnetization and mass change during the carburization of B-2 in H_2/CO (3/1). The data obtained at 598 K are of particular interest, since this temperature is well above the Curie points of the expected carbide products (Hagg Fe_2C and Fe_3C), but well below that of the starting material (metallic iron). Consequently the magnetization results provide a measure of the number of iron atoms remaining as metallic iron in the sample without interference from iron carbide phases, and the mass increase indicates the number of carbon atoms added to the sample. The relationship between magnetization and mass increase is shown in Figure 4 in a plot of the fraction of α -iron atoms in the sample (ordinate) versus the number of carbon atoms added to the sample per atom of iron in all phases (abscissa). These results indicate that magnetization initially drops sharply, then becomes less steep as carburization proceeds. Extrapolation of the initial slope suggests that during the early stage each carbon atom is associated with about 8 iron atoms. Subsequently, as more carbon atoms are added to the system, the resulting curve extrapolates to a stoichiometry of $\text{Fe}_{2.14}\text{C}$. Since TMA of the final sample indicates the presence

of Hagg carbide and a small amount of Fe_3C , we conclude that the stoichiometry of Hagg carbide is closer to Fe_2C than to $\text{Fe}_{2.5}\text{C}$, as suggested by Senateur et al.⁵ from the similarity of the x-ray pattern to Mn_5C_2 .^{5,6}

Long-term carburization experiments indicate that stoichiometric Fe_2C is reached before noncarbide carbon species begin to build up (Figure 3). This conclusion is important, since the known initial product of Fischer-Tropsch catalysis is methane and higher hydrocarbons follow only after several days of operation.⁷ Since Fe_2C reacts with hydrogen to form methane, the formation of noncarbide carbon species, which leads to the well known phenomenon of catalyst swelling, is very likely the intermediate in Fischer-Tropsch synthesis.

The TMA results for the carburized catalysts provide additional information on phase transformations that may occur during reduction and carburization. The TMA results for B-6 during long-term carburization (Table 6) indicate that during carburization the small amount of cementite (Fe_3C) that was formed initially together with the Hagg carbide was slowly converted to Hagg carbide. However, cementite is the stable phase to which Hagg carbide decomposes when heated to ~ 900 K. These results suggest that cementite can act as an intermediate in the carburization of iron to Hagg carbide.

The TMA results might be a useful indicator of crystallite sintering, assuming that the observed increases in magnetization are caused by growth of ferromagnetic domain size. To evaluate semiquantitatively the effect of carburization conditions on particle size, we have applied a simplified analysis to the magnetization force of the iron carbide phases observed. From the ratio of the magnetization force of the carbide phase per milligram of catalyst to the fractional mass content of the carbide, we may derive a normalized force due to magnetization per milligram Fe_2C . Comparison of the normalized forces so derived

offers a measure of ferromagnetic domain size. This analysis has been applied to the Hagg carbide phases of catalysts B-2 and B-6. The results show that at approximately comparable carburization conditions, the normalized magnetization for B-6 is larger than that for B-2 (Table 8). To interpret these results, we will assume for a given carburization condition that the calculated normalized magnetization force of the two catalysts is affected predominantly by differences in domain size rather than by compositional effects. On this basis, we conclude that carburization of B-2 produces smaller iron carbide domains (smaller crystallites) than does carburization of B-6. Also, lower heating rates in the temperature-programmed carburization yields smaller domains (smaller crystallite) for both catalysts.

Crystallite size has been reported to affect Curie temperature, and in the case of nickel, smaller metal particles produce lower Curie temperature.⁸ In the case of the Fischer-Tropsch catalysts, the Curie temperature of the Fe_2C carbides is approximately 35 degrees lower for catalyst B-6 than for B-2. Accordingly, the crystallite size of B-6 is expected to be smaller than that of B-2, but this conclusion is the opposite of that obtained from the magnetization results discussed in the previous paragraph. Hence, it appears that the relationship between crystallite size and Curie temperature for the Fe_2C carbide is the opposite of that of nickel. For the long-term carburization of B-6, the results in Table 6 show that during the period of noncarbide carbon growth (26 to 72 hr), the total magnetization force and the sum of the amounts of the two carbides (Hagg and Fe_3C) remain constant. Hence, we may conclude that little sintering occurred.

The fused iron catalyst (CCI-C73-2-01), after carburization and use in synthesis for several days at 10 atm, contained a ferromagnetic component that was primarily Fe_3O_4 (Table 7). Identification was made by measurement of Curie temperatures and x-ray diffraction patterns. The

much greater magnetization of this catalyst sample ($0.26 \text{ dyne mg}^{-1}$) in contrast to that of the same catalyst carburized for only several hours ($0.0055 \text{ dyne mg}^{-1}$) could result from either an increase in the amount of Fe_3O_4 during long-term carburization,⁷ or an increase in the size of magnetic domains.

The Raney-iron catalyst used in Fischer-Tropsch synthesis for several days at 10 atm contained three ferromagnetic phases: Hagg carbide Fe_3O_4 , and $\alpha\text{-Fe}$. The low values of magnetization suggest the existence of either a small amount of each of these phases, or small ferromagnetic domains, as suggested by the Curie temperature (773 K), which is lower than the Curie temperatures observed for the fused iron catalysts (790 and 820 K). Also, the low value of magnetization of the Raney iron suggests the presence of small ferromagnetic domains that have not undergone appreciable sintering.

Finally, the carburization process leads to the formation of another ferromagnetic phase of low yield with a Curie temperature in the range 400 K to 435 K. This phase has not yet been identified, but potassium ferrite ($\text{K}_2\text{O}\cdot\text{Fe}_2\text{O}_3$), which has a Curie temperature at 423 K, is a likely candidate. Potassium oxide is added as a promoter in the preparation of catalysts B-2 and B-6. Perhaps the formation of the potassium-ferrite phase is responsible for the improved catalytic properties of the catalysts.

B. Chemical Activity of Surface Intermediates

In conjunction with our magnetic studies on bulk carburization of iron-based Fischer-Tropsch catalysts (see Section II-A, above), we initiated an examination of the surface reactivity of such carburized catalysts. In these measurements we are attempting to measure steady-state catalyst activity and to identify the buildup of carbon-containing

intermediate species on the surface of the catalyst by exposing the catalyst to hydrogen after different degrees of carburization in H_2/CO mixtures (3/1 by volume) and in CO.

A microreactor system was constructed that could be operated under continuous-flow (15 psi) or pulse-mode conditions (50 psig). The Fischer-Tropsch catalyst used in these studies was the iron-based Fischer-Tropsch catalyst B-6 supplied by PERC. A sample of catalyst (0.5 g) was first reduced in H_2 (15 hr at 623 K followed by 2 hr at 723 K), after which the temperature was adjusted to 573 K for carburization in the H_2/CO (3/1) gas mixture. Product content was determined by gas chromatography on a temperature-programmed silica-gel column. During 15 hr of carburization the product stream was found to contain CO_2 , CH_4 , C_2H_6 , C_2H_4 , C_3H_6 , and some higher-molecular-weight hydrocarbons, some of which condensed at the exit from the reactor. CO conversion was nearly constant at a level of about 35 vol%.

Carburization of B-6 in H_2/CO (3/1) at 673 K resulted in a marked change in its appearance, characterized by a large increase in volume, or "swelling". At the same time, the CO consumption rose markedly to 100%. Under these conditions, the product composition had changed to CH_4 , CO_2 , C_2H_6 , and C_3H_8 (in order of decreasing yield). The production of olefins and higher molecular weight hydrocarbons appeared to have ceased. For B-6 catalyst carburized at 673 K, the product distribution as a function of reaction temperature is given in Figure 5. Although CO_2 formation shows little change with temperature, the production of C_1 - to C_3 - hydrocarbons exhibits maxima near 623 K for CH_4 and near 573 K for C_2H_6 and C_3H_8 .

Carburization of B-6 in CO/He mixtures (rather than CO/H_2) at 673 K did not result in "swelling" or formation of Fischer-Tropsch products. On subsequent pulsing with H_2 methane was the only product observed.

Physical measurements by x-ray diffraction and magnetic susceptibility indicate that different bulk phases are present in the B-6 as a result of carburization in CO/He or CO/H₂ gas mixtures at 673 K, as shown in the following table.

Carburization Gas	X-Ray Diffraction	Magnetic Susceptibility
CO/H ₂	Fe ₂ C (Hagg), crystalline carbon	Fe ₂ C (Hagg)
CO/He	Fe ₃ C, cementite	Fe ₃ C (cementite)*

* Small contribution due to Fe₂C (Hagg) observed.

A mass spectrometer was used to test the reactivity in hydrogen of B-6 catalyst samples pretreated in these different ways. A sample of the catalyst was placed in a microreactor and hydrogen was flowed through it. The effluent from the reactor was sampled by the mass spectrometer, which rapidly and repetitively scanned through the mass range for C₁ to C₉ hydrocarbons while the catalyst temperature was programmed linearly from 293 to 770 K.

Samples of B-6 catalyst examined in this way included one sample carburized in H₂/CO (3/1 by volume) at 573 K, one sample carburized and "swelled" in H₂/CO (3/1) at 673 K, and one sample carburized in CO at 673 K. In all cases, methane was the only product observed. As for the surface composition of B-6 before and after carburization in H₂/CO at 673 K, we find from CO-adsorption measurements at 298 K that the freshly reduced catalyst adsorbs 2.76×10^{-6} moles of CO per gram of catalyst, whereas "swelled" catalyst does not adsorb CO. Thus, metallic iron crystallites may no longer be present on the carburized catalyst surface, possibly because of the formation of the carbon-hydrogen intermediate adlayer.

Our experimental studies, although preliminary and qualitative, lead us to conclude that Fe_2C is the active catalyst for the Fischer-Tropsch synthesis over iron catalysts. This material, which seems to be formed by exposure of B-2 and B-6 catalysts only to CO/H_2 mixtures, promotes the growth of surface intermediates required for the formation of high molecular weight products. A layer of Fe_2C probably forms rapidly near the surface of the catalyst. Carbon-containing surface species then grow on top of the Fe_2C layer, causing the catalyst to swell. When these carbonaceous surface adsorbates interact with hydrogen and carbon monoxide, hydrocarbon production results.

C. Carbon Deposition Boundaries for the C-H-O System in the Presence of Iron

In our current studies of the interaction of H_2/CO gas mixtures with iron-based Fischer-Tropsch catalysts, we have recognized the importance of thermodynamic properties of the C-Fe-O system. Although information is available on the carbon (graphite) deposition boundaries for this system over a range of temperatures and pressures,⁹ the thermodynamic equilibria involving the iron oxides and carbides as solid phases have received less attention. That these solid phases exist has been recognized earlier and confirmed in our experimental work on carburization of catalysts B-2 and B-6. In a recent study of Manning,¹⁰ the thermodynamic calculations include Fe and Fe_3O_4 as stable phases in equilibrium with H_2O , CO , CH_4 , and CO_2 . We have reproduced in Figure 6 the results of his calculations at 723 K and 1 atmosphere. Curve P-Q represents the phase boundary below which Fe_3O_4 is stable and above which Fe is the stable phase. Curve R-S indicates the phase boundary above which carbon (graphite) deposition occurs. Point X marks the feed gas composition $\text{H}_2/\text{CO} = 3/1$ (by volume). It is apparent that the formation of Fe_3O_4 and of carbon (graphite) would be favored thermodynamically.

The phase diagram for this system at lower temperature (573 K), as used in our carburization studies, is not available at the present time. Calculation of the thermodynamic stability diagrams at lower temperatures and in the presence of the carbides of iron would contribute greatly to our understanding of catalyst pretreatment in Fischer-Tropsch synthesis.

III METHANOL-SYNTHESIS CATALYSTS--SURFACE SULFIDATION AND SEGREGATION

Our measurements of the interaction of hydrogen sulfide with the surfaces of methanol-synthesis catalyst components¹ pointed to copper as the primary gateway for the rapid accumulation of surface sulfur. The possibility of transport of surface sulfur from the copper to the zinc oxide phases of the catalyst would depend on the degree of intermingling of the phases and on the mobility of the sulfur adatoms.

To gain some insight into the surface distribution of the catalyst components, a specimen of the CCI-C79-1 catalyst was examined by scanning electron microscopy (SEM).^{*} The specimen was in the form of a wafer reduced in hydrogen and subsequently exposed to H₂S/H₂ mixtures during Auger electron spectroscopy (AES) measurements. The same specimen was then exposed to the ambient atmosphere during transfer from AES to SEM. In addition to micrographic examination to reveal the structure of the surface, energy dispersive x-ray analysis was used to reveal the lateral distribution of the major surface components. The results (Figure 7) indicate that the Al₂O₃ phase is dispersed throughout a matrix in which it is not possible to differentiate between Cu and Zn phases, within the limit of resolution of the instrument. Cu and Zn are quite obviously in intimate proximity on the catalyst surface.

We are currently evaluating quantitatively the mobility of sulfur adatoms on a copper surface. By a movable shutter, which partially intercepts an argon ion beam, selective ion sputtering will be used to

* We are grateful to Dr. P. H. Holloway of Sandia Laboratories for the SEM micrographs of our catalyst specimen.

produce a sharp discontinuity in a sulfur adlayer on a copper foil specimen. We may then use Auger electron spectroscopy to monitor the rate of transport of surface sulfur from the saturated to the clean region of the copper as a function of specimen temperature. The activation energy for surface diffusion may be evaluated from such measurements. In addition, we will obtain surface sulfur concentration profiles by measuring the sulfur AES line intensity at multiple points on the surface at a discrete time interval after producing the discontinuity or after raising the temperature of the specimen. Changes in the surface sulfur concentration gradient will permit us to estimate the value of the coefficient of surface diffusion. The experimental setup for these measurements has been completed.

IV FUTURE WORK

During the next reporting period, we will place particular emphasis on problems related to the formation and role of bulk and surface carbon in Fischer-Tropsch catalysts. Specifically, we will continue to explore the effect of syn-gas composition on carbon take-up of the iron-based catalysts, and will carburize catalyst samples at high-pressure (150 psi). Specimens of these catalysts will be examined by TMA and exposed to temperature-programmed desorption experiments. In addition, we will determine the depth of carbon deposit and the distribution of promoters by Auger electron spectroscopy in conjunction with argon ion etching. Also, our studies will be extended to include some ruthenium-based catalysts supplied by PERC.

V REFERENCES

1. SRI Quarterly Progress Report No. 5 (PERC-0060-5).
2. R. A. Diffenbach, ERDA-PERC (private communication).
3. L.J.E. Hofer and A. M. Cohn, *Anal. Chem.* 22, 907 (1950).
4. J. L. Falconer and R. J. Madix, *Surf. Sci.* 48, 393 (1975).
5. J. F. Senateur, R. Fruchart, and A. Michel, *Compt. Rend.* 255, 1615 (1962).
6. K. H. Jack and S. Wilde, *Nature*, 212, 248 (1966).
7. H. H. Storch, N. Golumbic, and R. B. Anderson, "The Fischer-Tropsch and Related Syntheses," (John Wiley and Sons, Inc., New York) 1951.
8. J. L. Carter and J. M. Sinfelt, *J. Catalysis* 10, 134 (1968).
9. A. D. Tevebaugh and E. J. Caires, *J. Chem. Eng. Data* 10, 359 (1965).
10. M. P. Manning "An Investigation of the Bosch Process," Ph.D. Thesis, 1976, Massachusetts Institute of Technology.

Table 1
 REDUCTION OF CATALYSTS B-2 AND B-6 IN
 100% H₂ AT 1 ATMOSPHERE

Catalyst	Reduction temperature (K)	Rate of temperature rise (K/hr)	Temperature of maximum rate of mass loss T _{max} (K)	Mass lost during reduction ^a (wt%)
B-2	450 to 735	17.1 ± 0.1	697 ± 2	18.8 ± 0.5
	450 to 735	17.7 ± 0.1	704 ± 2	19.3 ± 0.5
	450 to 735	18.3 ± 0.1	712 ± 2	18.7 ± 0.5
	465 to 755	19.1 ± 0.1	709 ± 2	18.7 ± 0.5
	460 to 781	19.1 ± 0.1	716 ± 2	19.5 ± 0.5
B-6	440 to 730	17.3	665	21.7
	450 to 760	17.9	667	21.7
	440 to 730	18.8	684	22.2

^aWith respect to mass of unreduced catalyst.

Table 2

ISOTHERMAL CARBURIZATION STUDIES WITH
FISCHER-TROPSCH CATALYSTS

Temperature (°C)	Catalyst	H ₂ /CO (by vol.)	Parabolic Rate Constant (wt% min ^{-1/2})	
			Region I	Region II
481	B-2	3/1	0.15	-
573	B-2	3/1	0.78	0.18
598	B-2	3/1	1.85	0.19
573	B-6	3/1	0.78	0.43
573	B-6	1.5/1	0.78	0.44

Table 3

TEMPERATURE-PROGRAMMED CARBURIZATION
STUDIES WITH CATALYSTS B-2 AND B-6

Catalyst	Rate of temperature rise (K/min)	Mass gain ^a (wt%)	Fractional Conversion to Fe ₂ C (wt%)
B-2	0.42	6.6	62
B-2	0.63	6.4	60
B-6	0.37	6.2	58
B-6	0.55	6.6	62

Table 4

OBSERVED CURIE TEMPERATURES AND
PROBABLE ASSIGNMENTS TO FERROMAGNETIC PHASES

Curie Temperature (K)		Ferromagnetic Phase
Observed Range	Literature ¹	
400-435	423	$K_2O \cdot Fe_2O_3$
484-493	478-493	Fe_3C
520-572	520-549	Fe_2C (Hagg)
635-685	653	Fe_2C (Hexagonal)
773-820	838-868	Fe_3O_4

Table 5

THERMOMAGNETIC ANALYSIS OF FISCHER-TROPSCH
CATALYSTS B-2 AND B-6 AFTER SHORT-TERM CARBURIZATION

Catalyst	Carburization			Ferromagnetic Phase Composition (wt%)				
	Temperature (K)	Time (hr)	H ₂ /CO (vol%)	K ₂ O-Fe ₂ O ₃	Fe ₃ C	Fe ₂ C (Hagg)	Fe ₂ C (Hexagonal)	α-Fe
B-2	598	1.3	3/1	6	3	88	0	3
B-2	573	4.0	3/1	4	0	95	0	1
B-2	481	5.0	3/1	0	0	0	80	20
B-2	440 to 590 ^a (0.42 K min ⁻¹)	6.0	3/1	4	0	84	0	12
B-2	420 to 590 ^a (0.63 K min ⁻¹)	4.5	3/1	5	0	84	0	11
B-6	573	3.0	1.5/1	0	17	69	0	14
B-6	432 to 580 ^a (0.37 K min ⁻¹)	6.6	3/1	6	0	81	0	13
B-6	443 to 598 ^a (0.55 K min ⁻¹)	4.7	3/1	10	22	60	0	8
B-6 ^b	573 (573 to 673)	4.0 56.7	3/1	4	0	96	0	0

^aTemperature-programmed; rate of temperature rise in parenthesis.

^bCarburization performed in separate apparatus.

Table 6

THERMOMAGNETIC ANALYSIS OF FISCHER-TROPSCH
CATALYST B-6 AFTER LONG TERM CARBURIZATION

Carburization Temperature (K)	Total Exposure Time ^a (hr)	Carburization to FeC ₂ ^b (%)	Total Magnetization Force ^c (dynes/mg sample) × 10 ²	Ferromagnetic-Phase Composition (wt%)				
				K ₂ O·F ₂ O ₃	Fe ₃ C	Fe ₂ C (Hagg)	Fe ₂ C (Hexagonal)	α-Fe
443 to 598	5	62	72	10	22	60	0	8
598	26	116	60	8	11	81	0	0
598	47	148	59	6	0	91	0	0
598	72	133	59	6	0	94	0	0

^a Gas composition: H₂/CO = 3/1.

^b Percent of total mass increase relative to that required to form stoichiometric Fe₂C.

^c At 300 K.

Table 7
 THERMOMAGNETIC STUDIES OF USED FISCHER-TROPSCH
 CATALYSTS

Catalyst Sample	Catalyst History	Ferromagnetic Components					
		Fe ₂ C (Hagg)		Fe ₃ O ₄		α -Fe	
		(wt%)	Curie Temperature (K)	(wt%)	Curie Temperature (K)	(wt%)	Curie Temperature (K)
Raney Iron	H ₂ /CO (3/1) at 10 atm, ~ 600 K, several days	26	540	70	773	4	> 850
Fused Iron CCI-C73-2-01	H ₂ /CO (3/1) at 10 atm, ~ 600 K, several days	-	-	100 ^b	790	-	-
Fused Iron CCI-C73-2-01	H ₂ /CO (3/1) at 20 atm, several hours	-	-	55	820	45	> 900
B-6 ^a	r ₂ /CO (3/1) at 1 atm, 575 to 675 K, 2 1/2 days	100	543	-	-	-	-

^a See Figure 3 and Table 6 of this report.

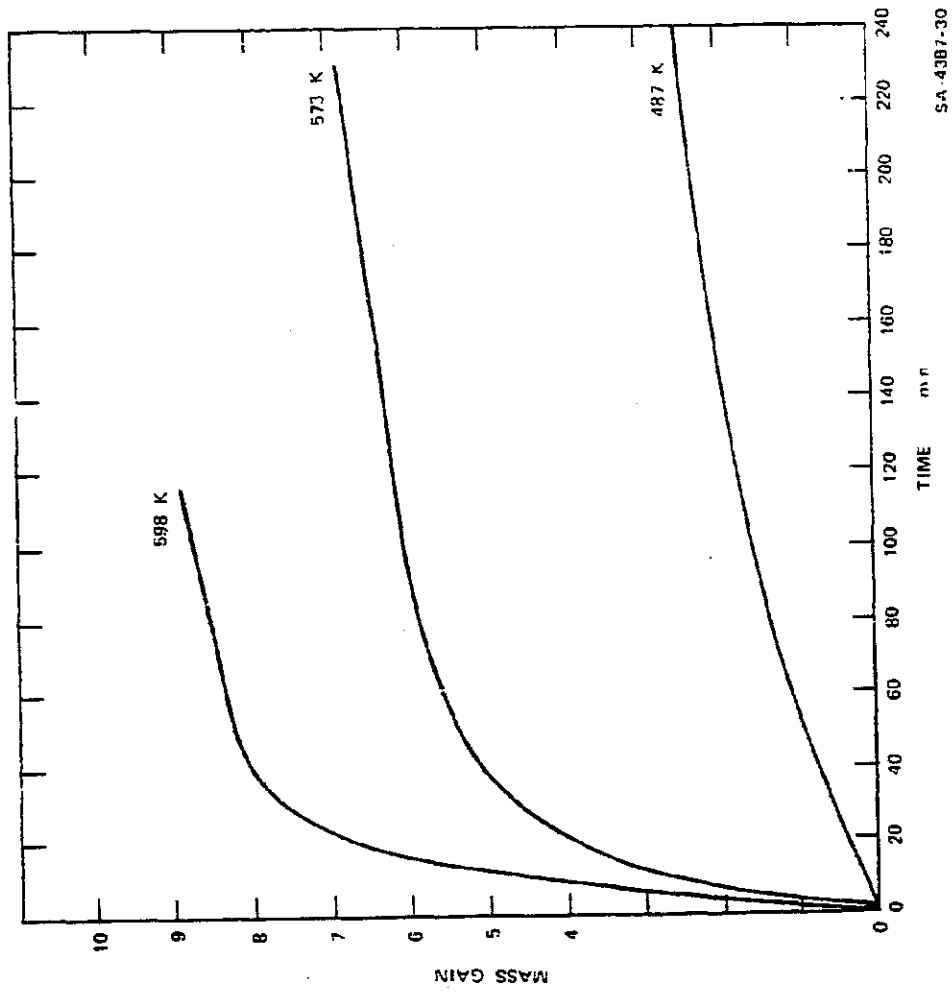
^b Fe₃O₄-phase confirmed by x-ray diffraction.

Table 8

INTERPRETATION OF THERMOMAGNETIC MEASUREMENTS

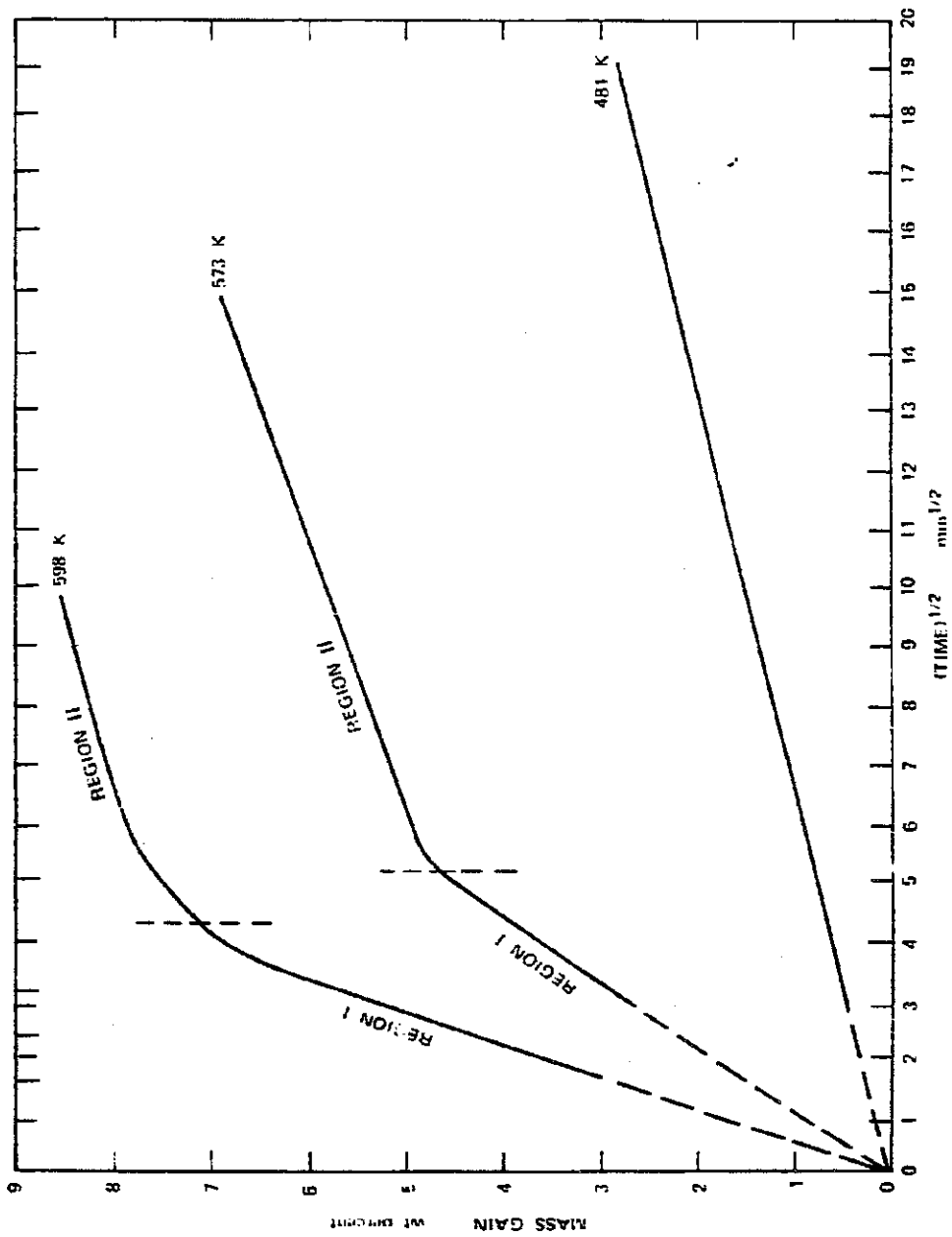
Catalyst	Carburization Process				H ₂ /CO (by vol)	Hagg Carbide Magnetization Force (dyne mg ⁻¹ Fe ₂ C) x 10 ²
	Isothermal		Non-Isothermal			
	Temperature (K)	Time (hr)	Temperature Range (K)	Heating Rate (K·min ⁻¹)		
B-2	598	1.3	-	-	3/1	5.9
B-2	573	4.0	-	-	3/1	4.6
B-2	-	-	441-590	0.42	3/1	5.9
B-2	-	-	420-588	0.63	3/1	20.5
B-6	-	-	432-580	0.37	3/1	7.2
B-6	-	-	443-598	0.55	3/1	56
B-6 ^a	-	-	448-570	1.00	3/1	135
B-6 ^b	573	3	-	-	3/1	51
	573-623	21				

^a Reference (1)^b Carburization performed in separate apparatus.



SA-43B7-30

FIGURE 1 MASS GAIN OF CATALYST B-2 DURING CARBURIZATION IN H₂ CO 3:1 AT 1 ATM



SA 4387-31

FIGURE 2 PARABOLIC PLOT OF MASS GAIN OF CATALYST B-2 DURING CARBURIZATION IN H₂/CO = 3/1 AT 1 ATM

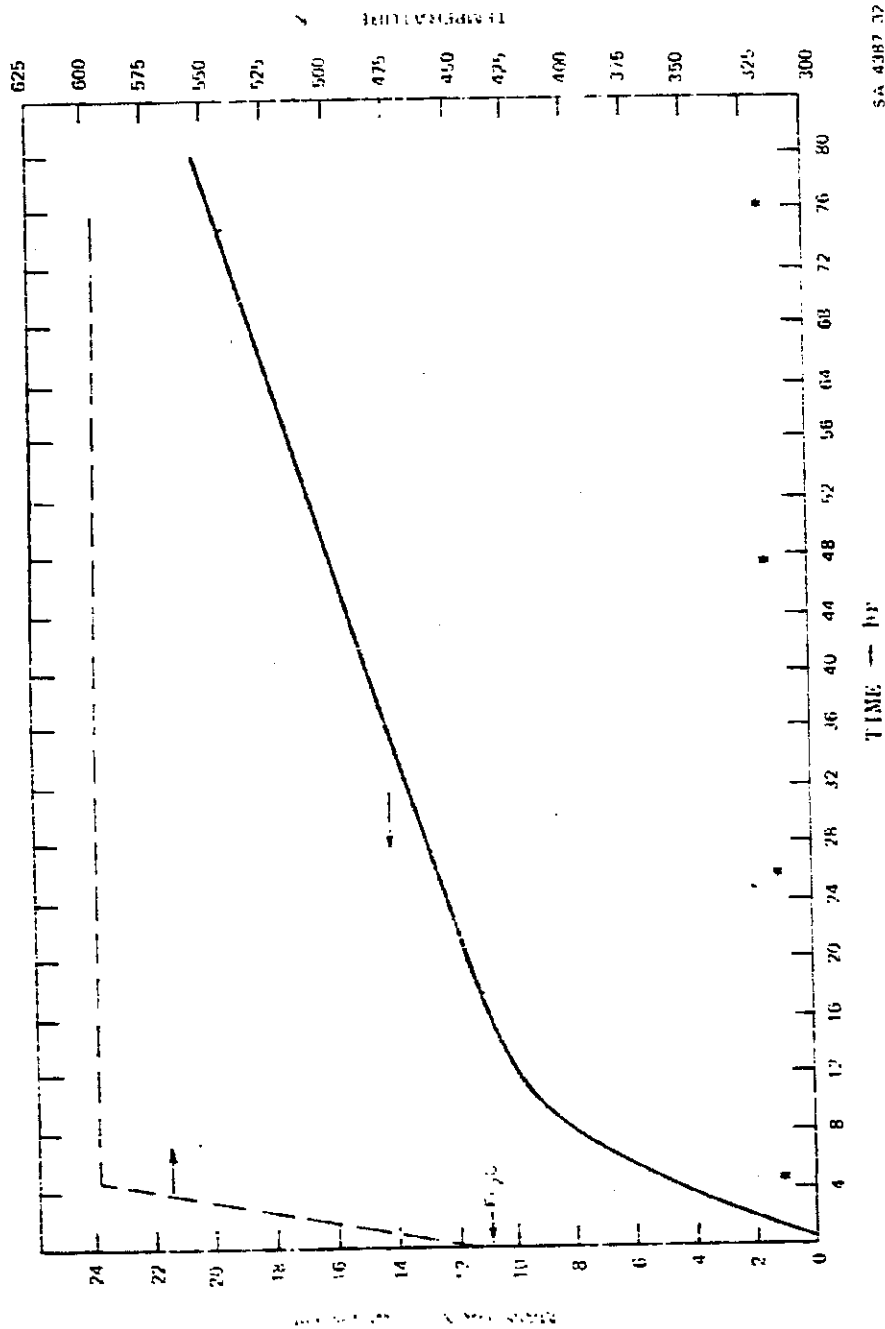


FIGURE 3 MASS GAIN OF CATALYST B-2 DURING LONG-TERM CARBURIZATION IN H₂ CO - 3:1 AT 1 ATM
 (Indicates time at which thermomagnetic analysis was made)

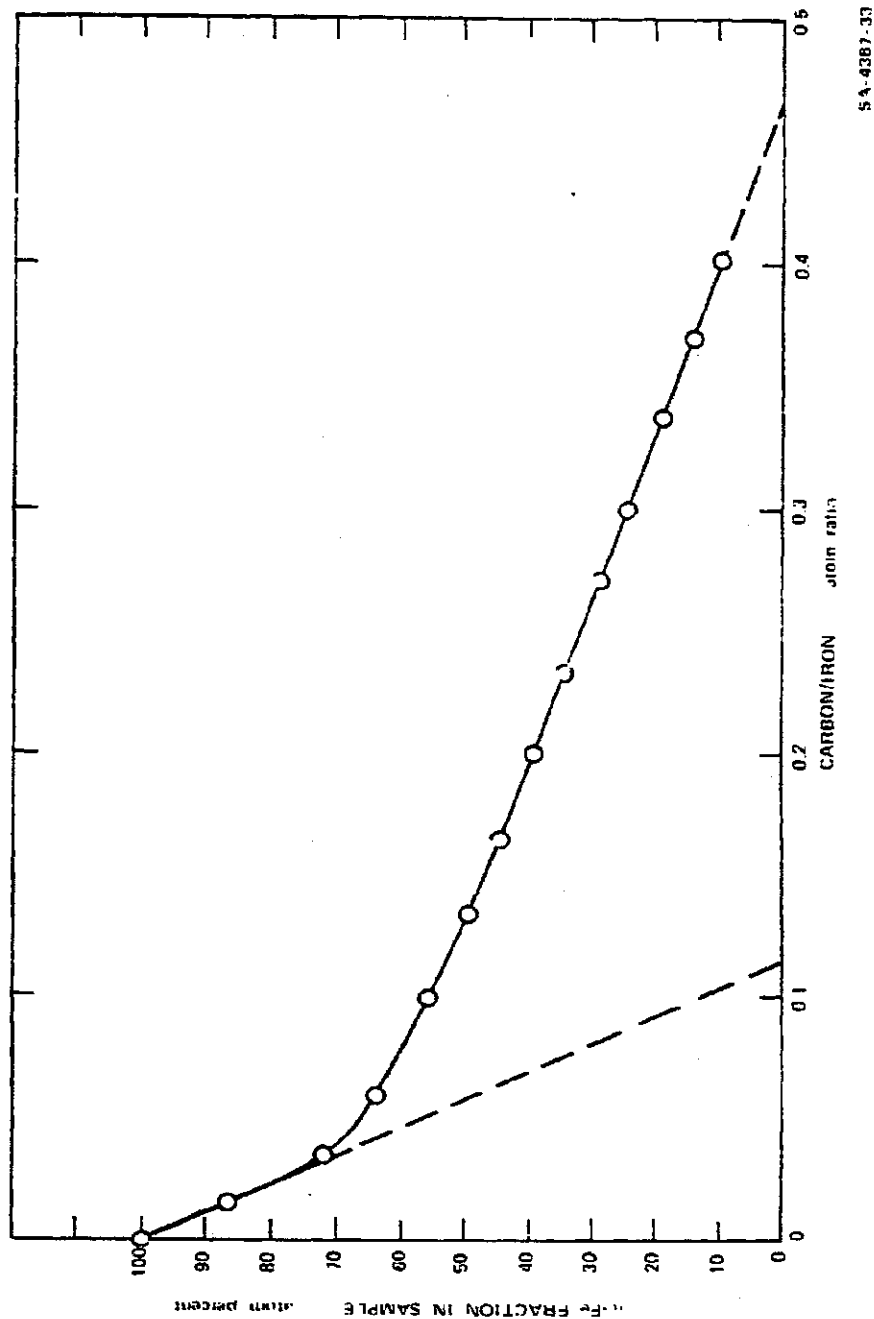


FIGURE 4 PERCENT IRON AS A FUNCTION OF CARBON/IRON RATIO DURING CARBURIZATION OF CATALYST B-2 AT 598 K
 Values on ordinate and abscissa derived from magnetization and mass gain data, respectively.

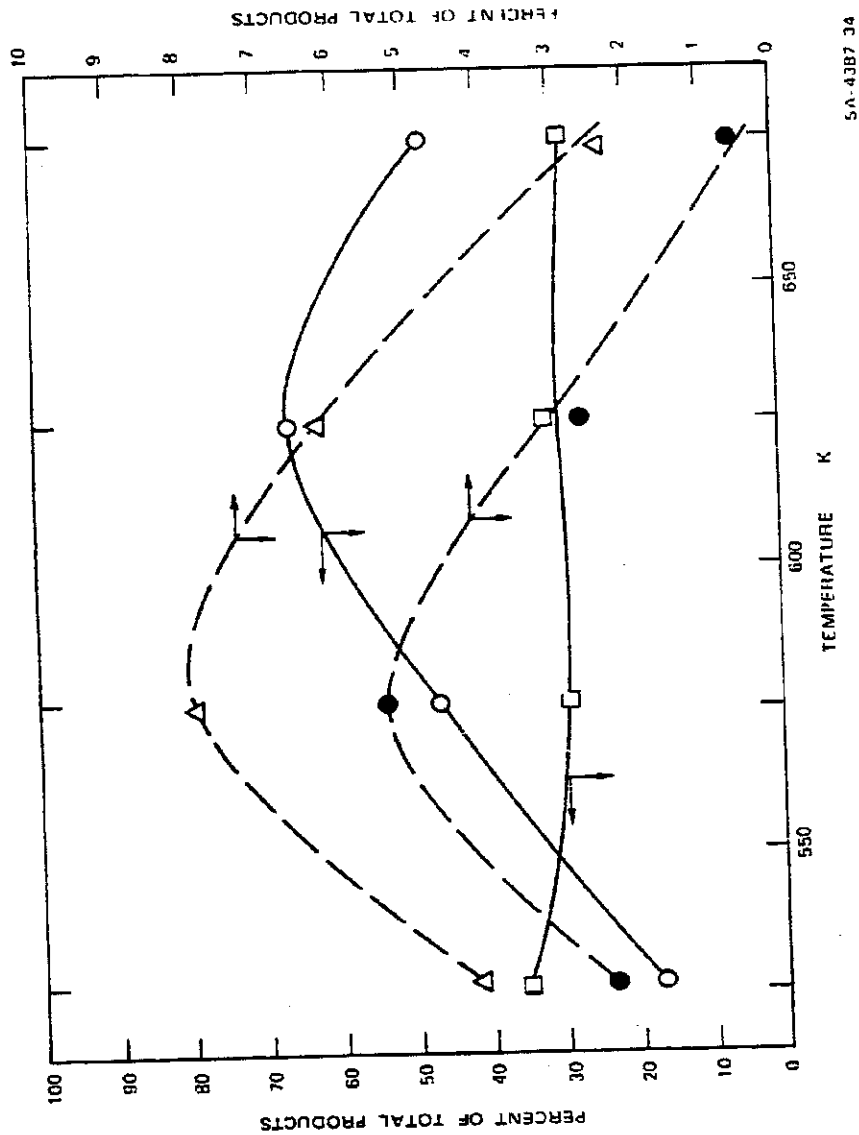
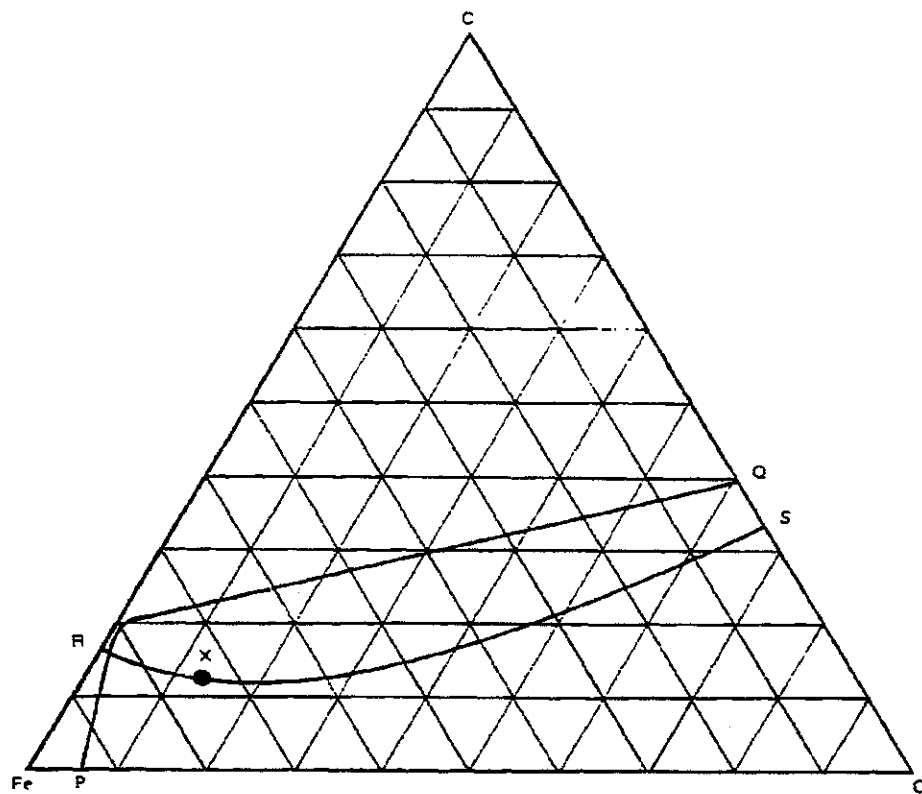


FIGURE 5 PRODUCT DISTRIBUTION AS A FUNCTION OF TEMPERATURE. CATALYST B-6
 CARBURIZED IN H₂:CO = 3 AT 673 K

Feed gas: 3/1 H₂:CO; flow rate: 20 cm³ min. Percent of CO consumed = 100%.

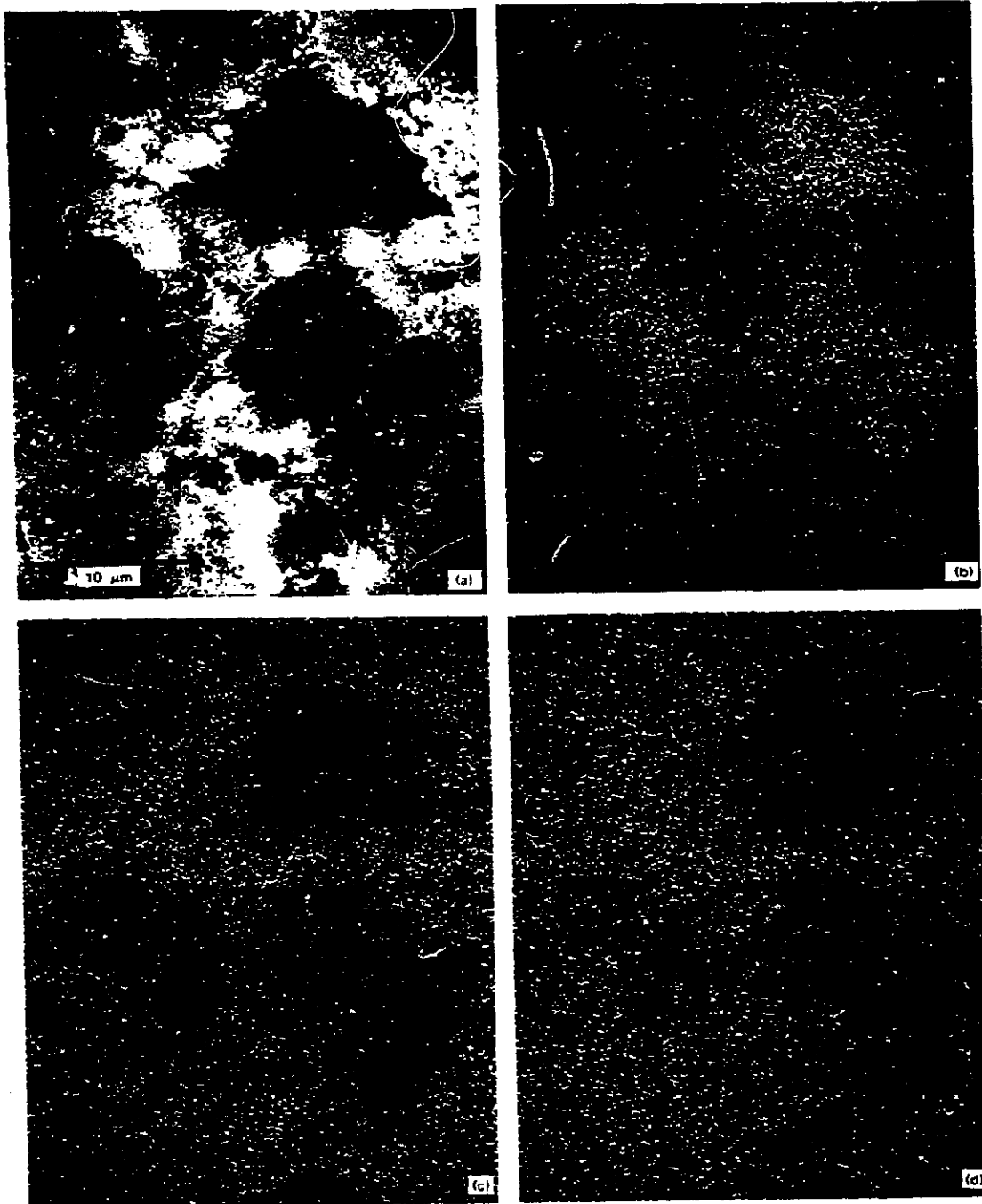
○ CH₄; □ CO₂; △ C₂H₆; ● C₃H₈



SOURCE M. P. Manning, "An Investigation of the Bosch Process", Ph.D Thesis, M.I.T., 1976

SA-4387-35

FIGURE 6 IRON - OXYGEN - GRAPHITE PHASE DIAGRAM
723 K, 1 ATM



SA-4387-36

FIGURE 7 SCANNING ELECTRON MICROGRAPHS OF PRESSED WAFER OF C79-1 METHANOL SYNTHESIS CATALYST

Dark regions in micrograph A are revealed to be particles of Al_2O_3 immersed in a Cu/Zn matrix by the x-ray maps for Al (B), Zn (C), and Cu (D).